COMPARISON OF CONVENTIONAL AND TYPE CURVE ANALYSIS OF PRESSURE FALLOFF TESTING FOR A CARBONATE RESERVOIR

Duane A. Crawford
Texas Tech University

ABSTRACT

This paper discusses the comparison of conventional transient analysis and type curve analysis (Hadinoto-Raghavan) in computing reservoir parameters for a West Texas carbonate reservoir using pressure falloff data taken from moderately fractured water injection wells.

The theory and application of conventional analysis and type curve analysis to pressure falloff testing are discussed. Included are example calculations showing excellent agreement in computing water formation capacity, k_wh, and fracture length, x_f, using the two methods.

INTRODUCTION

A study of pressure falloff test (PFOT) analysis was made on field data taken from a San Andres carbonate reservoir. The purpose of the study was to evaluate water formation capacity, k_wh, and fracture length, x_f, and other parameters using multiple PFOT data taken from 104 moderately stimulated injectors using conventional transient analysis, then comparing with recent type curve techniques. For the 606 tests available, 322 were conducive to analysis. Striking agreement was obtained for k_wh and x_f values between methods and for multiple tests of the various injectors.

THEORY

Flow Behavior

Fluid flow from a vertically fractured well into the reservoir goes through three flow regimes:

1. - lateral linear flow from the fracture into the formation through the fracture faces
2. - elliptical flow as the streamlines yield to the more radially-formed equipotential lines established in non-fractured portions of the reservoir
3. - pseudo-radial flow as elliptical configuration yields to radial geometry.

These modes of flow are strongly influenced by the equipotential field out to where half the pressure drop occurs. This region comprises one half the area of the producer-injector pattern, i.e., the constant pressure boundary of the flow circumscribed by this half-area as depicted in Figure No. 1.

Regimes No. 1 and No. 2 are dominated by transient flow behavior. Regime No. 3 has a more stabilized flow in accordance with pseudo-radial flow behavior.

Fractures

Within a given pattern, vertical injection well fractures can be either favorably or unfavorably oriented. The two extremes are:

1. fractures oriented from injector to injector (unfavorable), and
2. fractures oriented from injector to producer (favorable).

These orientations are shown in Figure No. 2. Fracture orientation is of secondary importance if the fractures are short.

CONVENTIONAL TRANSIENT ANALYSIS USING NEW TECHNIQUES

Conventional determination of $k_w h$ is based on:

$$k_w h = \frac{162.6\ i_w\ \mu_w\ B_w}{m} \tag{1}$$

for porous, permeable, radial non-fractured reservoir geometries. The slope m may be taken from a Miller-Dyes-Hutchinson plot (log Δt vs P). The presence of a fracture requires a trial-and-error solution to correct the slope, i.e.:

$$(k_w h)_c = \frac{162.6\ i_w\ \mu_w\ B_w}{m_c} \tag{2}$$

which is to say:

$$\frac{k_w h}{(k_w h)_c} = \frac{m}{m_c} \tag{3}$$

In order to calculate the corrected slope, m_c, the fracture length, x_f, must first be determined by:

$$x_f = \frac{0.391}{m_1}\sqrt{\frac{i_w\ m_c\ B_w}{\phi h\ C_t}} \tag{4}$$

which assumes an infinite conductivity fracture (no pressure loss in fracture). The slope, m_1, is taken from the square-root of time plot after comparing the log ΔP vs log Δt plot. Each of these plots show any early-time linear flow, following any skin and/or afterflow, with linear flow (hence fracture flow) ceasing at the same time on each plot. The slope, m_c, is calculated by iteration assuming trial fracture lengths and using the Hadinoto-Raghavan slope correction plot with equation no. 4:

$$m_{c_{trial}} = \frac{m}{(Kh)_t/(Kh)_a \quad trial} \tag{5}$$

Calculation of the corrected semilog slope, m_c, originated with Russell and Truitt using a plot of $(Kh)_{true}/(Kh)_{apparent}$ vs x_f/x_e, and was illustrated by Smith and Cobb.[1,2] For this study, the curves of Hadinoto and Raghavan were used because they are designed for constant-pressure square boundary conditions.[3,4] Figure No. 3 shows the Hadinoto-Raghavan slope correction plot (Reference No. 3) and its application to short fractures regardless of orientation, i.e., if x_f/x_e is less than 0.67. Fracture lengths for the subject reservoir were all short. Consequently, this slope correction curve was used throughout the study. In order to use the plot the dimensionless time at the start of pseudo-steady state flow, t_{DA}, is required:

$$t_{DA} = \frac{2.637 \times 10^{-4} k_w\ t}{C_t\ \phi\ \mu_w\ A} \tag{6}$$

For this study, the t_{DA} values exceeded 0.1 (using the most conservative k_w and t values) permitting use of just one curve on the plot (emphasized in Figure No. 3). The slope, corrected in this manner, is used in equation no. 2 to calculate $(k_w h)_c$.

The computation of x_f thus leads to m_c yielding $(k_wh)_c$. The corrected slope, m_c, is then pivoted through the last portion of late time data on the MDH plot to predict the falloff pressure at one hour, $P_{1\ HR,\ CORR}$, as shown in Figure No. 4 and the total skin is calculated using:

$$S = 1.151 \left[\frac{(P_{wf} - P_{1\ HR,\ CORR})}{m_c} - \log \frac{(k_w h)_c}{(\phi h)(\mu_w)(C_t)(r_w)^2} + 3.23 \right] \quad (7)$$

From this step, skin damage can be determined from:

$$S_{dam} = \frac{(P_{int} - P_{wf})}{141.2\ i_w\ B_w\ \mu_w} (k_w h)_c \quad (8)$$

where P_{int} is read at time zero, from the square-root plot, as the m_1 slope intercept (see Figure No. 5).

If skin due to partial penetration, perforations, turbulence and wellbore slant can be ignored:

$$S_{frac} = S - S_{dam} \quad (9)$$

These assumptions were appropriate for the injectors studied.

Finally, condition ratio may be calculated from:

$$CR = \frac{\ln (r_e/r_w)}{\ln (r_e/r_w) + S} \quad (10)$$

as a measure of well efficiency. Here, $r_e = r_{hd}$ after fillup or $r_e = r_{ob}$ prior to fillup.

TYPE CURVE ANALYSIS

Type curve analysis provides a quick method of calculating reservoir parameters while circumventing the need to find corrected slopes by iteration. The Hadinoto-Raghavan curves are designed to handle square constant-pressure boundary problems such as exist in many waterflood patterns. The basic type curves are shown as Figure No. 6 (infinite capacity) and Figure No. 7 (uniform flux) and are extensions of the work by Gringarten et al.[5] The upward trending x_e/x_f lines are designed to handle boundaries and the lower set of curves are designed to handle flow behavior that has reached pseudo-steady-state conditions prior to reaching boundaries. The central curve (marked "infinity"), the type curve most often used in this study, represents a vertical fracture in an infinite system.

These type curves are plots of dimensionless pressure (ordinate equation):

$$P_{wD} = \frac{k_w h\ (P_i - P_{wf})}{141.2\ i_w\ \mu_w\ B_w} \quad (11)$$

and dimensionless time (abscissa equation):

$$t_D = \frac{2.64 \times 10^{-4}\ k_w\ t}{\phi\ \mu_w\ C_t\ (x_f)^2} \quad (12)$$

where this last equation was used in this study in the following form:

$$t_{D_{x_f}} = \frac{2.64 \times 10^{-4} (k_w h)_T \, t}{(\phi h) \, \mu_w \, C_t \, (x_f)^2} \tag{13}$$

Consequently, the curves allow match point correlation between real and dimensionless data to back-calculate $k_w h$ and x_f from equations (11) and (13).

The basic procedure is to plot pressure drop, psi, versus time, hours, on log-log paper at precisely the same log-cycle scale as the type curve. The real curve is shifted, horizontally and vertically, over the type curve until a curve match is achieved. Any combination of matching P_{wD} and t_D values may be taken from any intersection common to both plots. In this study, it was convenient to always match on $P_{wD} = 1$ and $t_D = 1$. These match points are then used to calculate $k_w h$ and x_f.

EXAMPLE CALCULATION

Conventional Analysis of Data

1. The following data were available for the example falloff test:

W_i = 1,006,000 cumulative barrels of injection water

ϕh = 12.432 fractional-feet

r_w = 0.1979 ft

μ_w = 0.65 cp

i_w = 636 BW/D stabilized (10 days) injection rate

S_{gi} = 15%

B_w = 1 RB/STB

$C_t = 10^{-5}$ psi^{-1}, assumed

A = 23.2 acres, grid area:

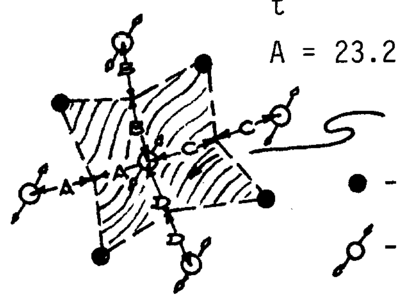

2. Half the distance between adjacent injectors, r_{hd}, averages:

$$r_{hd} = \sqrt{\frac{43560A}{2}} = \sqrt{\frac{23.2\text{ac} \times 43560 \text{ ft}^3/\text{ac-ft}}{2}} = 502.6 \text{ ft}$$

3. The radius of the oil-bank, r_{ob}, and percent fillup are:

$$r_{ob} = \sqrt{\frac{5.615 \, W_i}{\pi(\phi h) \, S_{gi}}} = \sqrt{\frac{5.615 \times 1.006 \times 10^6}{\pi(12.432)(0.15)}} = 982.0 \text{ ft}$$

$$\%FU = 100W_i/7758(\phi h) \, S_{gi} A$$

$$= 100 \times 1.006 \times 10^6/7758 \times 12.432 \times 0.15 \times 23.2 = 300\%$$

Since fillup exceeds 100%, r_{hd} is used in the calculations instead of r_{ob}.

4. From $\sqrt{\Delta t}$ vs P (Figure No. 5) and log Δt vs log ΔP (Figure No. 4) linear flow ceased in one hour. Afterflow was nil. The slope, m_1, taken through the best straight line that terminates at one hour on the $\sqrt{\Delta t}$ plot is 148 psi/$\sqrt{\text{hr}}$.
5. Pseudo-radial flow was evident after approximately 10 hours (one log cycle beyond

cessation of linear flow) with a slope, m = 336 psi/cycle, from the MDH plot (Figure No. 4).

6. Dimensionless time, t_{DA}, becomes:

$$t_{DA} = \frac{2.637 \times 10^{-4} \times 3.5 \times 240}{0.1 \times 10^{-5} \times 0.65 \times 23.2 \times 43560} = 0.56$$

which is greater than 0.1 allowing use of the Hadinoto-Raghavan plot (Figure No. 7). The value of 240 represents 10 days ≡ 240 hours, the average stabilization time used to control injection rates prior to PFOT shutin in this study. The 240 hours represents the minimum time required to establish pseudo-radial flow in the reservoir system tested.

7. A trial value of x_f = 78.2 ft was assumed, giving x_f/x_e = 78.2/502.6 = 0.156 which cross-plots on Figure No. 3 to give a value of $(kh)_t/(kh)_a$ = 0.927. Therefore, the corrected trial slope is:

$$m_c\text{, trial} = 336/0.927 - 361.9 \text{ psi/cycle}$$

and the new trial fracture length is:

$$(x_f)_{trial} = \frac{0.361}{148}\sqrt{\frac{636 \times 361.9 \times 1}{12.432 \times 10^{-5}}} = 93.0 \text{ ft.}$$

This calculation was repeated until:

$$(x_f)_{trial} = (x_f)_{calc}$$

Usually no more than two trials were required. The trial value of $x_{f\ trial}$ = 94 ft yielded a $x_{f\ calc}$ = 94 ft predicting:

$$m_c = 369.9 \text{ psi/cycle}$$

8. Consequently:

$$(k_w h)_c = 162.6 \times 636 \times 0.65 \times 1/369.9$$
$$= 181.7 \text{ md-ft}$$

and:

$$(k_w)_c = 181.7/112 = 1.62 \text{ md}$$

Type Curve Analysis of Data

1. By type curve match (Figure No. 8), a "fair-to-good" match was made using the real data and the uniform flux type curve (of Figure No. 7):

$$\text{at } P_{wD} = 1,\ (\Delta P)_M = 270 \text{ psia}$$

therefore:

$$(k_w h)_T = 141.2 \times 636 \times 0.65 \times 1/270 = 212.3 \text{ md-ft}$$

and:

$$\text{at } t_{D_{x_f}} = 1,\ (\Delta t)_M = 10 \text{ hr}$$

therefore:

$$(x_f)_T = \left[\frac{0.0002637 \times 213.3 \times 10}{12.432 \times 0.65 \times 10^{-5} \times 1}\right]^{1/2} = 78.2 \text{ ft}$$

2. For this example, a "fair" curve fit was also obtained using the infinite capacity type curve (of Figure No. 6) and:

$$\text{at } P_{wD} = 1, \ (\Delta P)_M = 275 \text{ psi}$$

therefore:

$$(k_w h)_T = 216.2 \text{ md-ft}$$

and:

$$(x_f)_T = 65.7 \text{ ft.}$$

For most of the injectors, in this study, the uniform flux curves had the better fits.

Other Calculations

Once $k_w h$ has been determined, skin and flow efficiency calculations are possible. In this study, these calculations were keyed to conventional analysis results.

1. Skin calculations were made by first ascertaining $P_{1 \text{ HR,CORR}}$ from m_c (shown in Figure No. 4). The total skin, for example, was:

$$S = 1.151 \left[\frac{P_{1 \text{ HR CORR}} - P_{wf}}{m_c} - \log \frac{(k_w h)_c}{\phi h \ \mu_w \ C_t \ r_w^2} + 3.23 \right]$$

$$= 1.51 \left[\frac{2971 - 3002}{369.9} - \log \frac{181.7}{12.432 \times 0.65 \times 10^{-5} \times (0.1979)^2} + 3.23 \right]$$

$$= -5.31$$

assuming skin damage due to well bore inclination, turbulence, pay penetration and perforations are nil:

$$S - S_{frac} = \frac{(P_{int} - P_{1 \text{ HR CORR}})}{141.2 \ i_w \ B_w \ \mu_w} \ (k_w h)_c \equiv S_{dam}$$

P_{int} = 2790 psig, the zero time intercept of the linear flow line (Figure No. 5) and:

$$S - S_{frac} = \frac{(2970 - 2971)(181.7)}{141.2 \times 636 \times 1 \times 0.65} = 0$$

$$S_{frac} = S - S_{dam} = -5.31 - 0 = -5.31$$

2. Flow efficiency can be measured by condition ratio:

$$CR = \frac{\ln (r_e/r_w)}{\ln (r_e/r_w) + S}$$

when $r_e = r_{hd}$ after fillup and $r_e = r_{ob}$ before fillup:

$$CR = \frac{\ln (502.6/0.1976)}{\ln (502.6/0.1976) - 5.31} = 3.10$$

Comparison of Data

The test results for this example are compared below:

	x_f, ft	$k_w h$, md-ft
conventional	94.0	181.7
type curve (uniform flux)	78.7	212.3
absolute error	19.4%	16.8%

Good agreement was obtained between the methods. Similar agreement was obtained from the other PFO tests on this well, confiming the data:

Test Time	$(k_w h)_C$	$(x_f)_C$	$(k_w h)_T$	$(x_f)_T$
1978 test (uniform flux)	181.7	94	216.2	78
1978 test (infinite capacity)	181.7	94	212.3	66
1975 test (uniform flux)	182.8	71	215.1	--
Average	182.3 md-ft	83 ft	215.7 md-ft	72 ft

Sequential $(k_w h)_C$ values agreed within 18.3% and sequential $(k_w h)_T$ values agreed within 17%. The overall agreement in fracture length was 15%.

Calculation Sequence

It was found advantageous, for routine calculations, to start with type curve analysis, using the $(x_f)_T$ data to enter into conventional analysis. This is because $(x_f)_T$ was found to be a reliable first approximation of $(x_f)_C$, reducing the trial-and-error procedure.

The close agreement found in sequential PFOT analysis and between conventional and type curve analysis suggests that the type curve analysis, alone, is reliable.

QUALITY OF DATA

$k_w h$ Data

Test results showed striking overall $k_w h$ agreement. Sequential values were arbitrarily required to agree within 25% to be valid:

$$\% \text{ agreement} = \frac{(k_w h)_{higher} - (k_w h)_{lower}}{(k_w h)_{lower}} \quad 100.$$

This agreement was also required in comparing $k_w h$ values calculated by the two methods. These data were then averaged to obtain single values of $(k_w h)_C$ and $(k_w h)_T$ for each injector. It was found that 63.5% of the averaged $k_w h$ data met the 25% criterion. For the total number of injectors, the averaged $k_w h$ data agreed much closer than 25%. Only 9.3% of the $(k_w h)_T$ values were found, from all tests, that exceeded 25% agreement. Only 5% of the tests failed to fit the type curves.

x_f Data

For the total number of wells having confirmed tests, 51% of them had fracture lengths that agreed within 25%.

Example Problem

The example test analysis included in this paper was selected as representative of mid-range agreement as outlined above. Numerous well tests could be cited that were in much closer agreement. Examples are shown below:

TEST PERIOD	$(k_wh)_C$	$(x_f)_C$	$(k_wh)_T$	$(x_f)_T$
8/1978 test	187.7	68	193.3	54
3/1978 test	202.2	65	210.6	67
1975 test	188.1	47	185.7	33
Average	192.7 md-ft	60 ft	196.5 md-ft	51 ft

Sequential $(k_wh)_C$ agreement is 2.0% and sequential $(k_wh)_T$ agreement is 2.8%.

SUMMARY

This paper sketches the results of PFOT analysis for moderately stimulated injectors in a San Andres carbonate reservoir and includes an example calculation procedure. In this study, recent state-of-the-art technology was used.

A considerable body of data was generated from this study that provides considerable support to the analytical techniques employed, particularly in verifying the type curve approach. The consistency and accuracy of k_wh results are considered remarkable and lend support to the agreement found in the computation of fracture length.

Fracture lengths were relatively short, as expected for the moderately stimulated injectors. No fracture lengthening trends were noted. Skin damage was of little consequence and total skin was invariably a large negative number. Skin, because of fracturing was usually close to the values found for total skin. Afterflow was essentially non-existant and linear flow was of minimal duration.

NOMENCLATURE

$m = 1/2$	The half slope that implies linear flow; from log ΔP versus log Δt plot.
$m = 1$	The unit slope that indicates afterflow; from log ΔP versus log Δt plot.
A	Area assigned to each injector by grid system developed for this report; acres
B_w	Formation volume factor for water, RB/STB, for this study.
C_t	Total compressibility of the system: $C_t = C_oS_o + C_wS_w + C_t$ for this study assumed $C_t = 10^{-5}$ psi^{-1}.
%FU	Percent of pattern filled up with injection water; area of pattern determined by grid system defined in report.
$(k_wh)_C$	Effective water permeability be net thickness or interwell water capacity, md-ft; by conventional analysis.
$(k_wh)_T$	Interwell water capacity, md-ft; by type curve analysis.
i_w	Injection rate, bbl/day

m	Original slope, psi/cycle, from semilog plot; taken during pseudo-radial flow time period.
m_1	Slope derived from pressure versus square root time plot; psi/$\sqrt{hr}$.
P_{wD}	Dimensionless pressure on type curves; corresponds to selected match point pressure $(\Delta P)_m$ in type curve fitting.
P_{wf}	Real shutin pressure of the injection well. For SEU wells this pressure measured at surface, -1350', and 4800' depth depending upon test.
r_{hd}	$\sqrt{A}/2$ for SEU patterns (for five-spot patterns this value is half the distance between paired injecotrs); ft.
r_{ob}	Radius of oil bank, ft; based on radial flow theory
r_w	Wellbore radius, ft.
S_{gi}	Initial gas saturation, 15% for this study.
Δt	Any subsequent cumulative shutin time, hrs.
$t_{D_{x_f}}$	Dimensionless time on fracture type curve; refers to dimensionless time corresponding to match point real time $(\Delta t)_M$.
$(\Delta t)_M$	Matching real time corresponding to $t_{D_{x_f}}$.
W_i	Cumulative water injection, bbl
x_e	Equals r_{ob} at less than 100% FU and equals r_{hd} at greater than 100% FU in the iterative solution for m_c and $(x_f)_c$; corresponds to $\sqrt{A}/2$ for gridded pattern used; corresponds to half the length of the side of a square pattern; ft.
x_f	Fracture length, wellbore to tip, ft; subscript "c" indicates fracture length calculated by conventional and iterative analysis; subscript "T" indicates fracture length determined by type curve analysis.
ϕh	Net porosity-feet per well
μ_w	Injection water viscosity, 0.65 cp for this study @ reservoir conditions.

REFERENCES

1. Russell, D. G., and Truitt, N. E., "Transient Pressure Behavior in Vertically Fractured Reservoirs", JPT (October, 1967).

2. Smith, J. T., and Cobb, W. M., "Application of Transient Pressure Analysis to Wells with Hydraulically Induced Vertical Fractures", Twenty-sixth Proceedings, Southwestern Petroleum Short Course, April, 1979, Texas Tech University.

3. Raghavan, R., and Hadinoto, N., "Analysis of Pressure Data for Fractured Wells:

The Constant Pressure Boundary", SPEJ (April, 1978).

4. Bennett, C. O., Reynolds, C., Jr., and Raghavan, R., "Analysis of Pressure Data from Vertically Fractured Injection Wells", SPE 8282 preprint, 54th Annual Meeting of the SPE, Las Vegas, Nevada, September 23-26, 1979.

5. Gringarten, A. D., Ramey, H. T., and Raghavan, R., "Applied Pressure Analysis for Fractured Wells", Trans of SPE of AIME (1975), v259, 888.

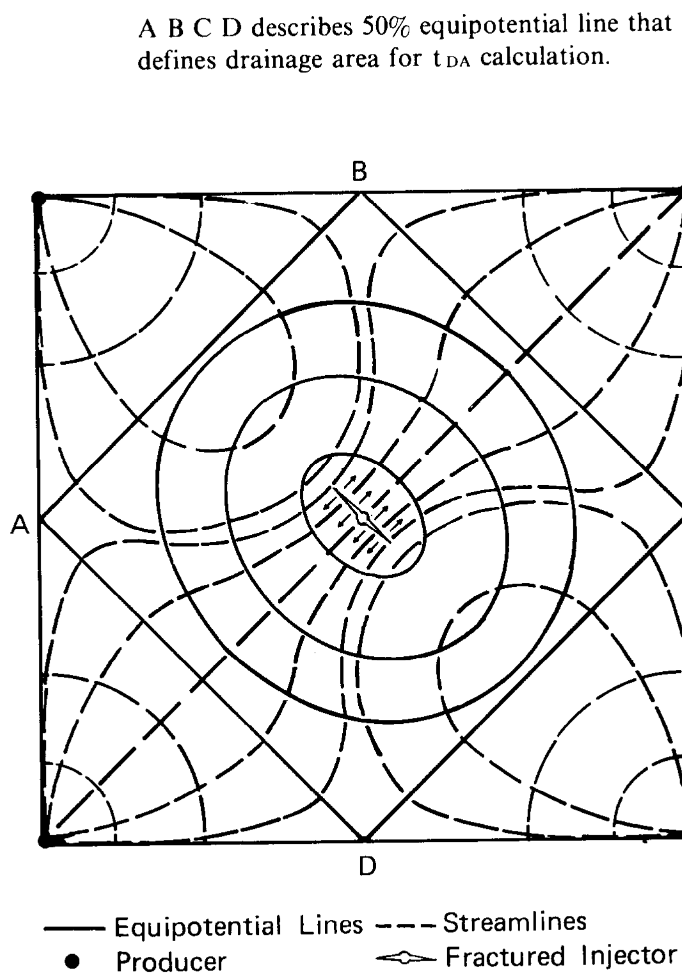

FIGURE NO. 1—REPRESENTATION OF FLOW REGIMES FOR FRACTURE FLOW IN SQUARE, CONSTANT-PRESSURE BOUNDARY PATTERN GEOMETRY (PRODUCER-TO-INJECTOR FRACTURE ORIENTATION SHOWN).

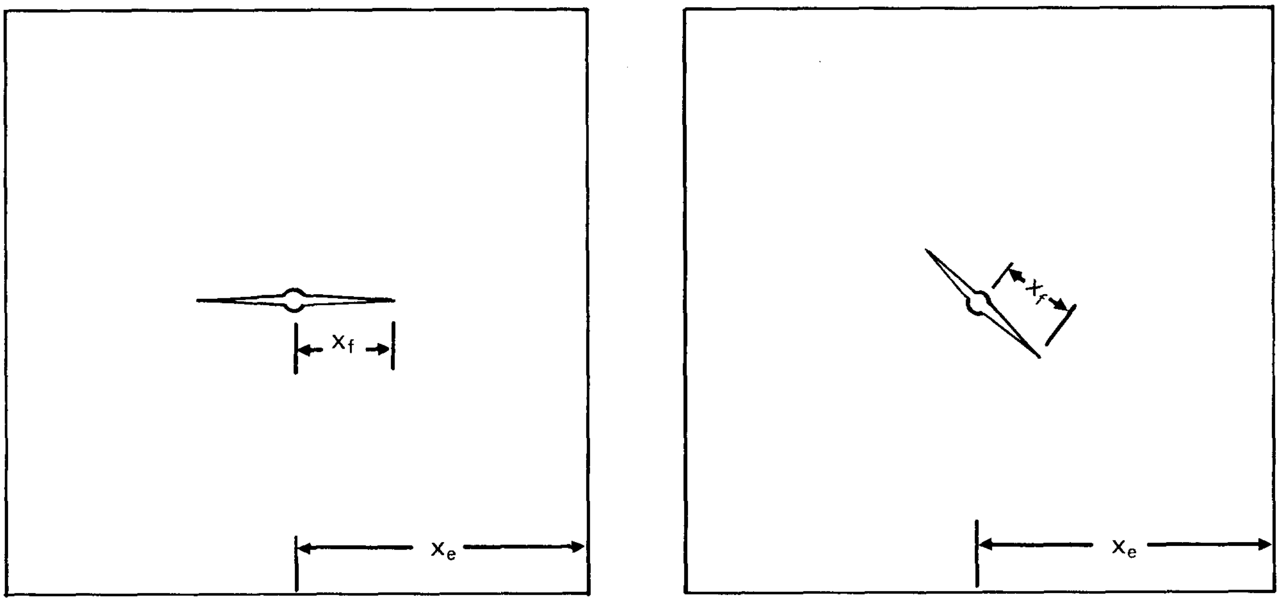

FIGURE NO. 2—TWO BASIC FRACTURE ORIENTATIONS ILLUSTRATED FOR A FIVE-SPOT PATTERN: (A) - UNFAVORABLE FRACTURE ORIENTATION, AND (B) - FAVORABLE FRACTURE ORIENTATION.

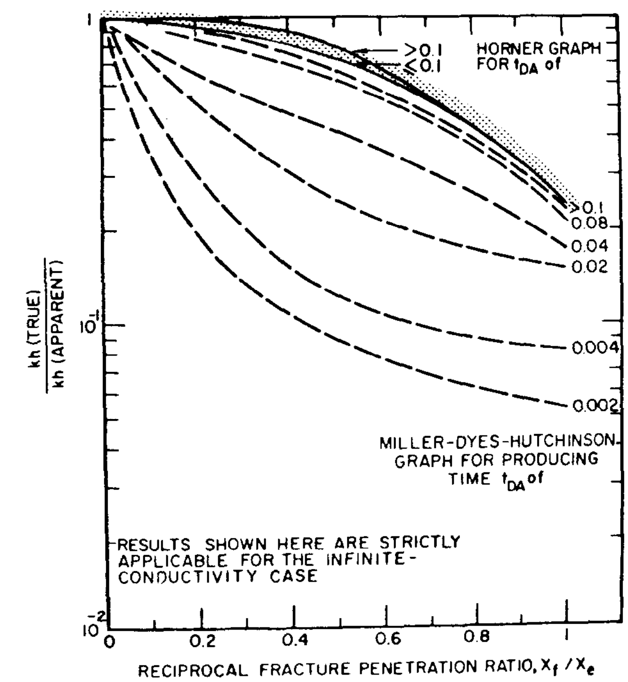

FIGURE NO. 3—TRUE TO APPARENT FORMATION CAPACITY VS RELATIVE FRACTURE LENGTH FOR VERTICALLY FRACTURED INJECTION WITH A CONSTANT PRESSURE BOUNDARY: CASE FOR $x_f/x_e<0.67$ (or $\sqrt{A}/2x_f \geq 1.5$) AND SQUARE BOUNDARY (VALID FOR FAVORABLE **AND** UNFAVORABLE FRACTURE OREINTATION). REFERENCE NO. 2.

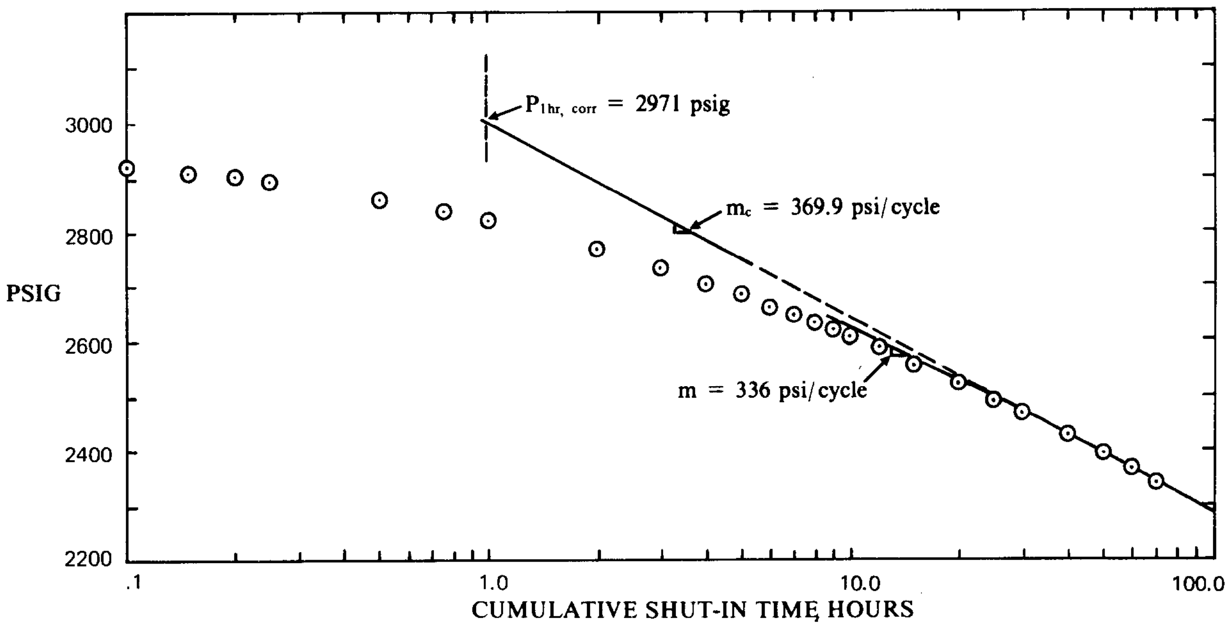

FIGURE NO. 4—MDH PLOT FOR EXAMPLE PROBLEM

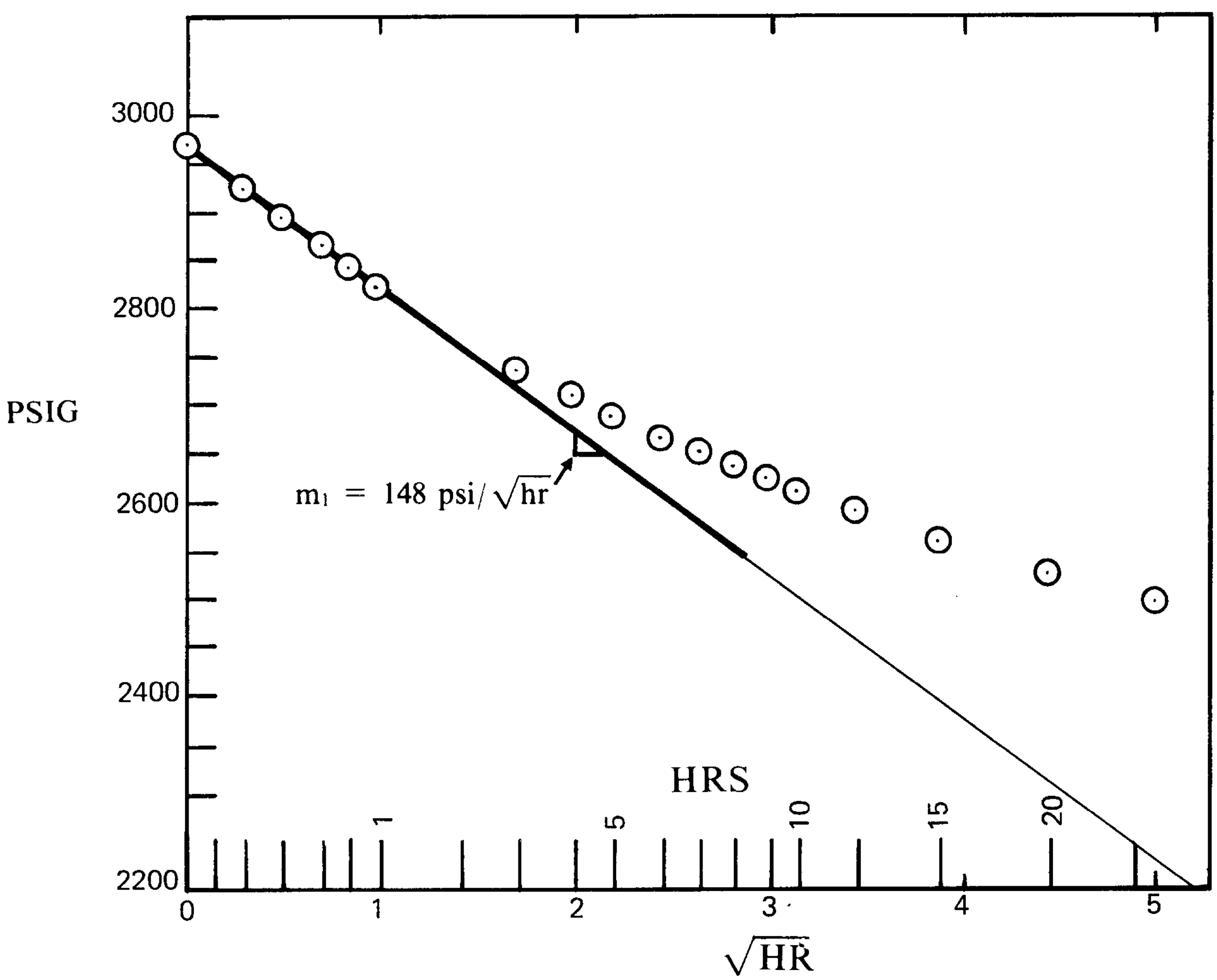

FIGURE NO. 5—SQUARE ROOT OF TIME PLOT FOR EXAMPLE PROBLEM.

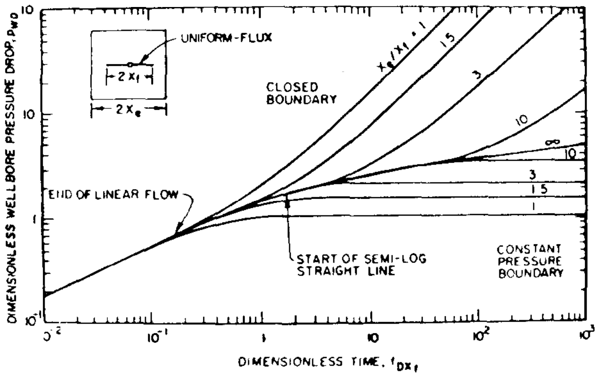

FIG. 7—DIMENSIONLESS WELLBORE PRESSURE DROP VS DIMENSIONLESS TIME FOR A UNIFORM-FLUX VERTICAL FRACTURE.

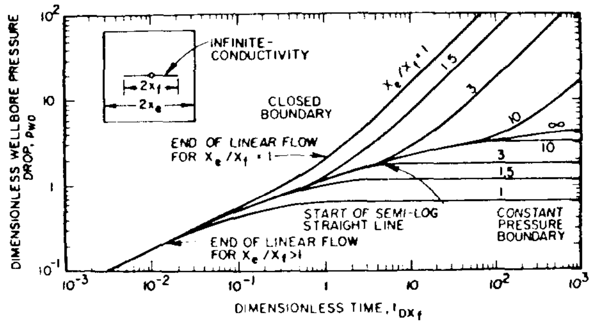

FIG. 6—DIMENSIONLESS WELLBORE PRESSURE DROP VS DIMENSIONLESS TIME FOR AN INFINITE-CONDUCTIVITY VERTICAL FRACTURE.

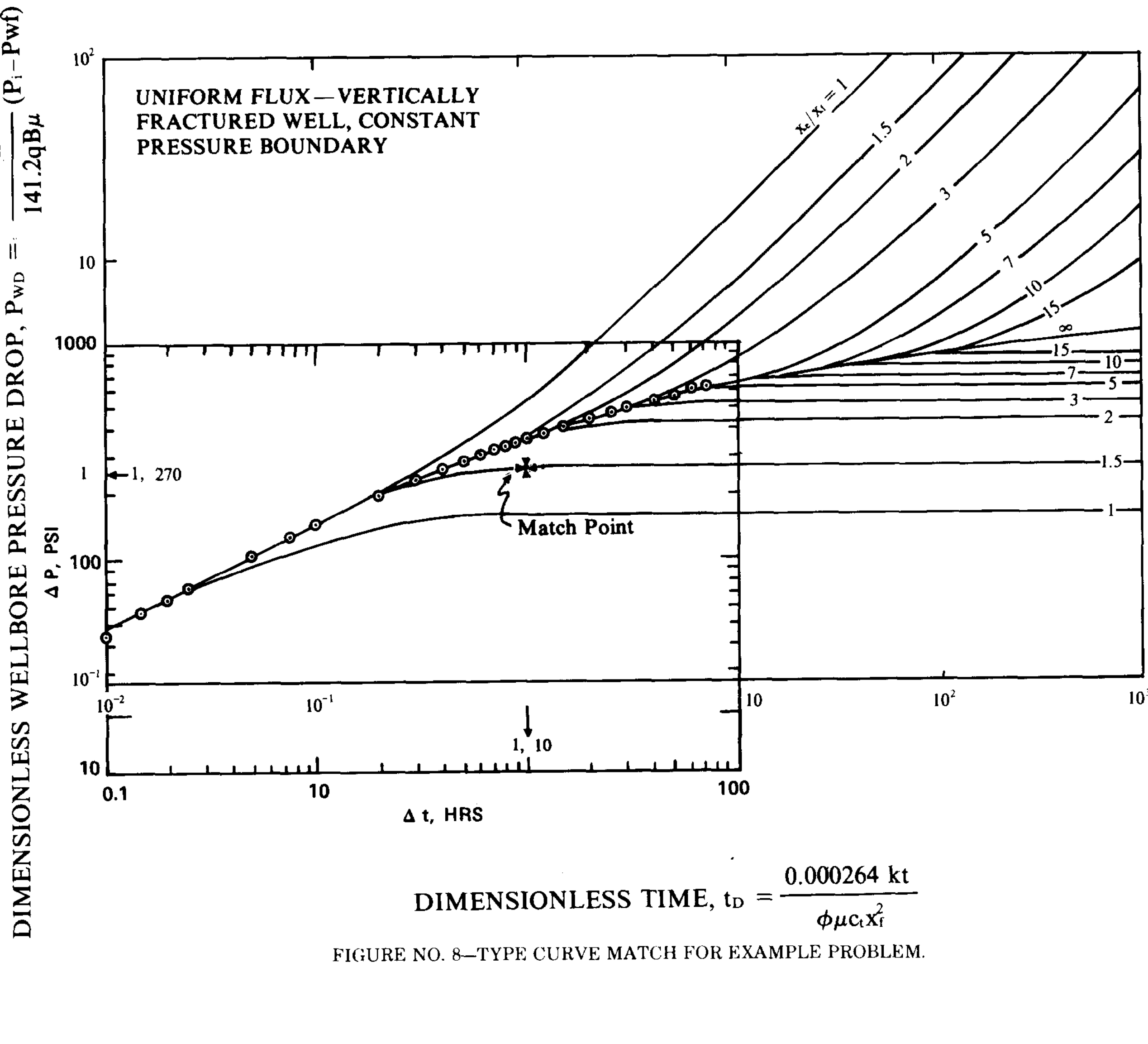

FIGURE NO. 8—TYPE CURVE MATCH FOR EXAMPLE PROBLEM.